Textile Fixed-Frequency Pattern-Reconfigurable Coupled-Mode Substrate-Integrated Cavity Antenna

Jie Cui, Feng-Xue Liu, Lei Zhao, *Senior Member IEEE,* Wenbin Dou, *Senior Member IEEE,*

***Abstract*—A textile fixed-frequency pattern-reconfigurabe coupled-mode substrate-integrated cavity (CMSIC) antenna is designed for wearable applications. The H-plane beam directions of the basic CMSIC antenna in the odd and even modes are theoretically deduced. Metallic snap buttons are added at the radiation apertures as switches. Simulations indicate that changing the state of the buttons leads to the shift of the odd- and even-mode resonance frequencies, and thus leads to the mode/pattern reconfiguration at 2.45 GHz. A textile prototype is fabricated using the computerized embroidery, and is measured to validate the design. The influences of human body and bending conditions are investigated through simulations and measurements.**

***Index Terms*—textile antenna, pattern reconfiguration, coupled mode, substrate-integrated cavity antenna.**

I. Introduction

Recently, the wearable antenna has been studied and applied in various areas including medical monitoring, sport, defense and security for its light weight, high flexibility and easy integration into clothes [1–4]. The wearable fixed-frequency pattern-reconfigurable antenna, usually loaded with switching diodes/varactors, has become a hot research topic because of its variable radiation characteristics at a fixed frequency. By changing the state of switches, the operating mode can be changed at a fixed frequency to switch its radiation pattern. The wearable microstrip antenna with a U-slot presented in [5] could realize three radiation patterns at 6.0 GHz. Reference [6] presented a microstrip patch antenna for WBAN applications with switchable patterns for the off-body and on-body links at 2.45 GHz. Reference [7] introduced a metamaterial-based wearable antenna with switchable broadside/omnidirectional patterns at 2.4 GHz. Besides, the wearable antennas proposed in reference [8, 9] can also achieve similar fixed-frequency radiation pattern reconfigurations.

The coupled-mode patch antennas (CMPAs) in [10–12] showed two resonance frequencies with different radiation patterns. Our previous work [13] also proposed a coupled-mode substrate-integrated cavity (CMSIC) antenna. By adding shorting pins at its two radiation apertures, the $|\mathrm{S}_{11}|$ curve can be shifted without deteriorating the impedance matching.

This letter is a more in-depth and targeted continuation of [13], and presents a practical geometry of a textile fixed-frequency pattern-reconfigurable CMSIC antenna with switching snap buttons. Firstly, its H-plane beam direction is theoretically deduced based on the directivity function of a two-element array. Secondly, simulations are carried out to determine the antenna dimensions and to study the influence of the human body on the antenna performance and the specific absorption rate (SAR) in the human body when the antenna is on the human body. Lastly, a textile prototype is fabricated and measured to verify the design and to investigate the robustness of the antenna against cylindrical bending conditions.

II. Theoretical Analysis

As shown in Fig. 1 (a), the basic CMSIC antenna can be considered as two back-to-back half-mode substrate-integrated cavities (HMSICs) with an aperture on the shared sidewall in between. A fundamental $\mathrm{TM}^{\mathrm{HM}}_{1,1,0}$ mode can excited in the the HMSIC with the feeding probe and coupled into the other HMSIC through the coupling aperture. Assuming that $l = 2w$ for simplicity, the resonance frequency f_r of the $\mathrm{TM}^{\mathrm{HM}}_{1,1,0}$ mode can be expressed as [14]:

$$f_r = \frac{c}{2\sqrt{\epsilon_r}}\sqrt{\frac{1}{4w^2}+\frac{1}{l^2}} = \frac{c}{2\sqrt{2\epsilon_r}w} \tag{1}$$

where c is the speed of light in the vacuum while ϵ_r represents the relative permittivity of the substrate.

According to the cavity model, the conducting part of the shared sidewall in the CMSIC antenna acts as PEC while the aperture on the sidewall acts as PMC. For the CMPA, the electric and magnetic couplings can be realized in its two bands and lead to the odd and even coupled modes, respectively [12]. The same dual-band/mode characteristic can be predicted in the similar geometry of the considered CMSIC antenna, and the E-fields can be co-phase or inverse-phase symmetrical at resonance frequencies. Each of two radiation apertures of the CMSIC antenna acts as a magnetic dipole. Without considering the ground plane, the radiation patterns of both dipoles are omnidirectional. Assuming their radiation

J. Cui is with the School of Information and Control Engineering, China University of Mining and Technology, Xuzhou, Jiangsu 221116, China and the School of Transportation Engineering, Jiangsu Vocational Institute of Architectural Technology, Xuzhou, Jiangsu 221116, China.

F.-X. Liu is with the School of Physics and Electronic Engineering, Jiangsu Normal University, Xuzhou, Jiangsu 221116, China and Jiangsu Normal University Kewen College, Xuzhou, Jiangsu 221132, China, and was with the State Key Laboratory of Millimeter Waves, Southeast University, Nanjing, Jiangsu 210096, China, when this work was performed.

L. Zhao is with the School of Information and Control Engineering, China University of Mining and Technology, Xuzhou, Jiangsu 221116, China.

W. Dou is with the State Key Laboratory of Millimeter Waves, Southeast University, Nanjing, Jiangsu 210096, China.

This work is supported by National Natural Science Foundation of China (61901457), Jiangsu College and University Natural Science Research Project (18KJB510014, 21KJB510030) and Xuzhou Science and Technology Project (KC19002).

Correspondence: liufengxue@jsnu.edu.cn (F.-X. L.); leizhao@jsnu.edu.cn (L. Z.).

Manuscript received XX XX, 202X; revised XX XX, 202X.

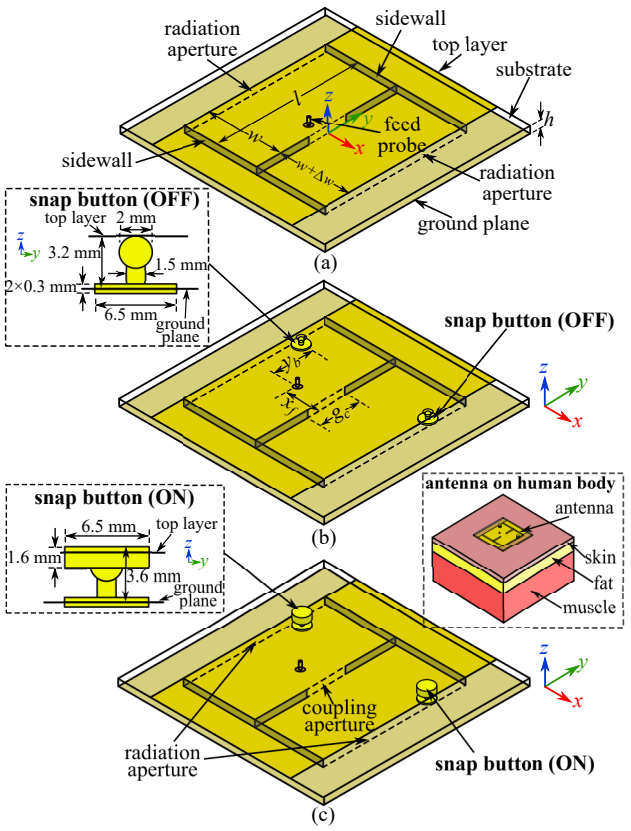

Fig. 1. Geometry of CMSIC antenna: (a) without snap buttons; (b) with buttons OFF; (c) with buttons ON.

powers are identical, the directivity function of the CMSIC antenna in the H-plane $F(\theta)$ can be expressed as:

$$F(\theta) = 2\cos\left(\frac{\pi}{\sqrt{2\epsilon_r}}\sin\theta + \frac{\Delta\varphi}{2}\right) \tag{2}$$

where $\Delta\varphi$ is the phase difference between two equivalent dipoles. For the even mode, $\Delta\varphi = 0$, and $|F(\theta)|$ reaches its maximum at $\theta = 0$, π. For the odd mode, $\Delta\varphi = \pi$, and θ can be theoretically calculated as:

$$\theta = \begin{cases} \pm\pi/2 & \epsilon_r \geqslant 2 \\ \pm\pi/2 \pm \arccos\sqrt{\epsilon_r/2} & \epsilon_r < 2 \end{cases} \tag{3}$$

III. Geometry and Materials

Fig. 1 (b) and (c) show the geometry of the CMSIC antenna loaded with two sets of copper snap buttons. Each set of button is composed by a removable female button and a male button installed on the ground plane. Two holes (radius r_h = 2 mm) are cut out from the top layer to avoid the direct shorting of the male buttons and the top layer when the female buttons are removed (buttons OFF). When the female buttons are pressed down (buttons ON), the whole buttons act as shorting pins. The substrate is made of the PF-4 foam sheet from Cuming Microwave with ϵ_r = 1.06, loss tangent $\tan\delta$ = 0.0001 and thickness h = 3.2 mm. The top layer and the ground plane (120×120 mm^2) are made of conductive fabric with a measured sheet resistance of 0.04 Ω/□. The sidewalls

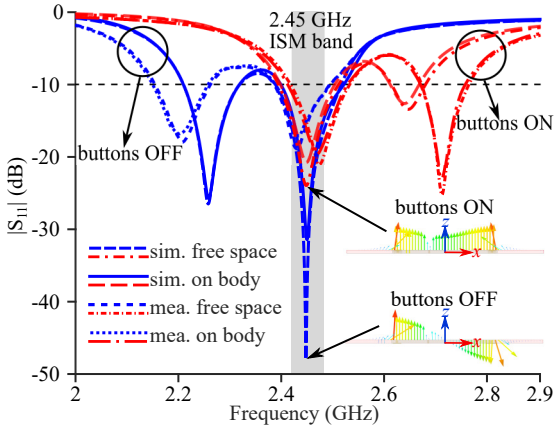

Fig. 2. Simulated and measured $|S_{11}|$ curves of proposed antenna in free space and on the human body.

are built by linear embroidery using conductive threads applied in 3 passes with a 2 mm stitching spacing, and are modelled as lossy planes with an equivalent sheet resistance of 0.7 Ω/□ according to empirical measurements.

Through simulations, the dimensions of the proposed antenna are optimized and determined as: l = $2w$ = 80.2 mm, Δw = -0.5 mm, x_f = 12.3 mm, g_c = 32.5 mm, y_b = 28 mm.

IV. Simulation Results

Two simulated $|S_{11}|$ curves of the proposed antenna with buttons OFF/ON in free space are shown in Fig. 2. A shift of the $|S_{11}|$ curve can be observed with buttons OFF/ON. Each of the curves show two resonance frequencies (lower f_{r1} and higher f_{r2}). The f_{r2} with buttons OFF and f_{r1} with buttons ON overlap with each other at 2.45 GHz, and both $|S_{11}|$ curves provide a coverage over the 2.45 GHz ISM band. Parameter studies (not shown for brevity) indicate that g_c determines f_{r1} without affecting f_{r2} for both scenarios, and y_b determines the shift amount of the button-ON $|S_{11}|$ curve with a stable Δf_r ($f_{r2} - f_{r1}$) while the button-OFF $|S_{11}|$ curve almost stays unchanged. The observed shift of the $|S_{11}|$ curve without significantly affecting the impedance matching can be explained by a detailed analysis over the equivalent circuit model. However, it can not be shown here because of the limited space of the letter, but will be carried out in the future works. As shown in the insets of Fig. 2, the simulated internal vector E-field distributions at 2.45 GHz prove that the antenna is operating in the even and odd modes with buttons OFF and ON, respectively.

The simulated 2.45 GHz co-polarized radiation patterns in free space are shown in Fig. 3. The H-plane patterns with buttons OFF and ON show noticeably different shapes. The button-OFF pattern is of a 10.1 dBi main beam close to the $+z$ axis ($\theta = -5°$, $-22 \sim 12°$ for half power) while the button-ON pattern is of a 7.1 dBi main beam at $\theta = -28°$ and a 6.2 dBi side lobe at $\theta = 42°$. Besides, the simulated radiation efficiencies are 95.9% and 91.2% with buttons OFF and ON, respectively.

The effects of a $300 \times 300 \times 60$ mm^3 three-layer (skin, fat and muscle) human body model on the antenna performance

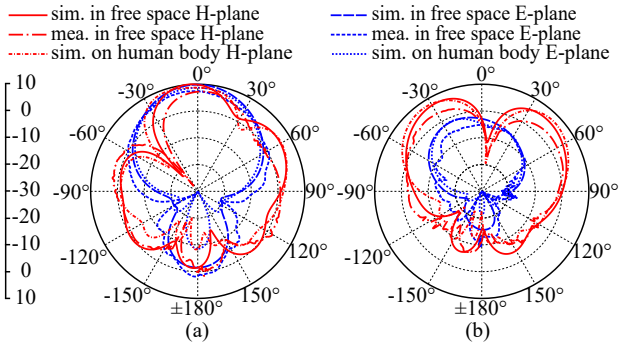

Fig. 3. Simulated and measured co-polarized radiation patterns of proposed antenna at 2.45 GHz: (a) buttons OFF; (b) buttons ON.

TABLE I
CHARACTERISTICS AND THICKNESSES OF SKIN, FAT AND MUSCLE

Layer	Relative permittivity	Conductivity (S/m)	Density (kg/m^3)	Thickness (mm)
Skin	38.09	1.43	1100	3
Fat	5.29	0.10	910	7
Muscle	52.82	1.69	1041	50

is studied through simulations. The thicknesses and characteristics at 2.45 GHz of each layers are listed in Table I [15]. As shown in the inset of Fig. 1, the antenna is located above the top center of the human body model with a 5 mm distance. The simulated $|S_{11}|$ curves of the proposed antenna on the human body model are shown Fig. 2. The agreement between the $|S_{11}|$ curves with/without the human body model indicates the sufficient isolation between antenna and human body.

The simulated 2.45 GHz co-polarized radiation patterns of the antenna on the human body model are shown in Fig. 3. The observed decrease of the backward radiation can be explained by the reflecting effect of the human body. With buttons OFF, the H-plane pattern shows a 9.1 dBi main beam close to the $+z$ axis ($\theta = -15°$, $-32 \sim 20°$ for half power). With buttons ON, the H-plane pattern shows a 7.9 dBi main beam at $\theta = -35°$ and a 7.4 dBi side lobe at $\theta = 46°$. And the simulated radiation efficiencies with buttons OFF and ON drop to 82.7% and 77.1%, respectively. This can be explained by the absorption of the human body as a lossy medium.

Figure 4 shows the simulated 1 g average SAR in the human body model with a 0.5 W input power at 2.45 GHz. The maximums of SAR are 0.14 and 0.17 W/kg with buttons OFF and ON, respectively. With a reduced d = 1 mm, they rise to 0.19 and 0.22 W/kg, but are still well below the limits of IEEE C95.1-2005 (1.6 W/kg) and of EN 50361-2001 (2.0 W/kg).

V. PROTOTYPE FABRICATION AND MEASUREMENTS

A prototype as shown in Fig. 5 is fabricated using a computerized embroidery machine (Brother NV950). The male buttons are manually installed on the ground plane for verification in this letter, and could be alternatively installed with embroidery techniques in the future mass production [16]. The measured $|S_{11}|$ curves of the prototype in free space and on the human body are shown in Fig. 2. The limited accuracy of the fabrication process leads to the differences between

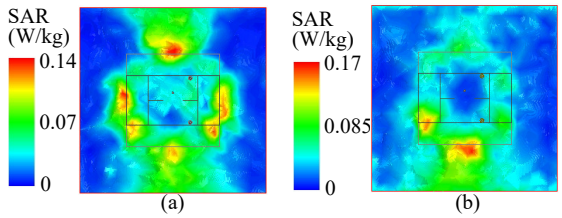

Fig. 4. Simulated 1 g average SAR in the human body model with a 0.5 W input power at 2.45 GHz: (a) buttons OFF; (b) buttons ON.

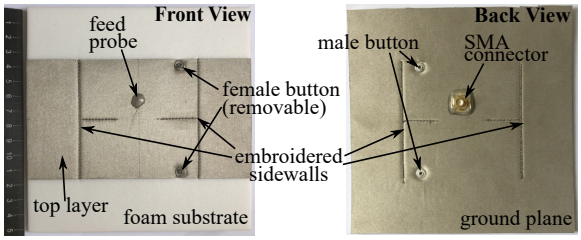

Fig. 5. Photos of fabricated prototype of propose antenna.

the measured and simulated $|S_{11}|$ curves. Minor shifts of the resonances at the 2.45 GHz with buttons OFF and ON in free space are observed, and the measured curves on the human body show high agreements with the free-space counterparts. With buttons OFF/ON in free space and on the human body, all four measured curves cover the 2.45 GHz ISM band, and $|S_{11}|$ is below -15 dB at 2.45 GHz.

The measured 2.45 GHz co-polarized radiation patterns of the prototype in free space are shown in Fig. 3. With buttons OFF, a 9.2 dBi main beam is observed at $\theta = -5°$ in H-plane. When the snap buttons are ON, the H-plane pattern shows a 3.8 dBi main beam at $\theta = -30.5°$ and a 3.1 dBi side lobe at $\theta = 42°$. Therefore, these measured patterns illustrate the expected fixed-frequency pattern-reconfigurable characteristic of the proposed antenna.

The prototype is also measured with cylindrical bending conditions in two directions as shown in the insets of Fig. 6. A PVC frame is fabricated to provide a suitable cylindrical surface with a 10.5 cm radius to imitate the bending conditions on the shoulder or limbs. Fig. 6 shows the measured $|S_{11}|$ curves with considered bending conditions. In direction 1, the button-OFF and button-ON curves basically overlap at 2.43 GHz. In direction 2, both measured curves show more shifts than that in direction 1. The measured $|S_{11}|$ at 2.45 GHz are still below -12.6 dB in bending conditions, and all measured $|S_{11}|$ curves with bending conditions can fully cover the 2.45 GHz ISM band.

Figure 7 shows the measured 2.45 GHz co-polarized radiation patterns of the proposed antenna with cylindrical bending conditions. Compared to the flat condition, the H-plane patterns, especially those with buttons OFF, show more deformations with bending in direction 2 than in direction 1. It further illustrates that bending in direction 2 leads to a greater impact on the radiation performance than that in direction 1. Therefore, when the antenna is located on the shoulder or limbs, it is better not to align the radiation apertures with the bending axis.

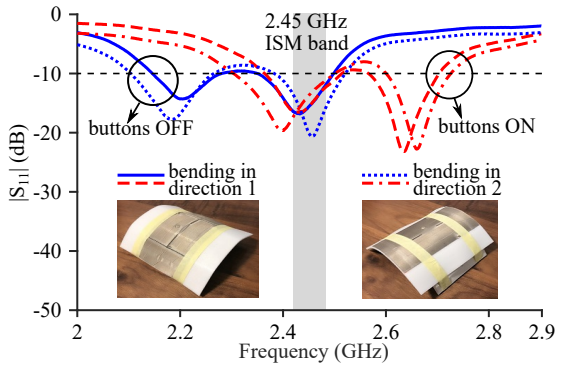

Fig. 6. Measured $|S_{11}|$ curves of proposed antenna with bending conditions (bending radius r_b = 10.5 cm).

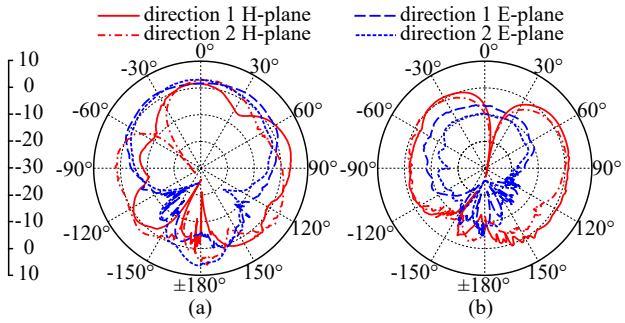

Fig. 7. Measured co-polarized radiation patterns of proposed antenna at 2.45 GHz with bending conditions: (a) buttons OFF; (b) buttons ON.

VI. Conclusion

A textile fixed-frequency pattern-reconfigurable CMSIC antenna has been designed and fabricated for wearable applications. The 2.45 GHz radiation pattern of the designed antenna can be reconfigured to be of a main beam close to the $+z$ axis for the off-body communication between the antenna and nearby data nodes (cellphone, etc.) with buttons OFF or two beams between the $+z$ axis and $\pm x$ axes for the on-body link between the antenna and other wearable equipment with buttons ON. In practical wearable applications in the wireless body-area network (WBAN), such pattern reconfiguration can be realized by mechanically pressing down or removing the female buttons instead of using a DC power with a limited battery capacity. Compared to the switching diodes/varactors, the snap buttons as switches are more compatible with textile materials, and require no soldering which can be vulnerable in bending conditions. Besides, the simulated SAR proves the safety of the proposed antenna on the human body, and the measured $|S_{11}|$ curves and radiation patterns indicate its robustness against bending conditions.

References

[1] A. Galehdar and D. V. Thiel, "Flexible, light-weight antenna at 2.4GHz for athlete clothing," in *Proc. APSURSI*, Honolulu, HI, USA, Dec, 2007, pp. 4160-4163.

[2] C. Hertleer, H. Rogier, L. Vallozzi and L. V. Langenhove, "A textile antenna for off-body communication integrated into protective clothing for firefighters," *IEEE Trans. Antennas Propag.*, vol. 57, no. 4, pp. 919–925, Apr. 2009.

[3] H. Lee, J. Tak and J. Choi, "Wearable antenna integrated into military berets for indoor/outdoor positioning system*IEEE Antennas Wireless Propag. Lett.*, vol. 16, pp.

[4] X. Lin, Y. Chen, Z. Gong, B.-C. Seet, L. Huang and Y. Lu, "Ultrawideband textile antenna for wearable microwave medical imaging applications," *IEEE Trans. Antennas Propag.*, vol. 68, no.6, pp. 4238–4249, Jun. 2020.

[5] S. Ha and C. W. Jung, "Reconfigurable beam steering using a microstrip patch antenna with a U-slot for wearable fabric applications," *IEEE Antennas Wireless Propag. Lett.*, vol. 10, pp. 1228-1231, Oct. 2011.

[6] A. R. Chandran, S. Morris, N. Timmons and J. Morrison, "Antenna with switchable propagating modes for WBAN applications," in *Proc. LAPC*, Loughborough, UK, Jan. 2015, pp. 1-3.

[7] S. Yan and G. A. E. Vandenbosch, "Radiation pattern-reconfigurable wearable antenna based on metamaterial structure," *IEEE Antennas Wireless Propag. Lett.*, vol. 15, pp. 1715-1718, Feb. 2016.

[8] H. Sun, Y. Hu, R. Ren, L. Zhao and F. Li, "Design of pattern-reconfigurable wearable antennas for body-centric communications," *IEEE Antennas Wireless Propag. Lett.*, vol. 19, no. 8, pp. 1385-1389, Aug. 2020.

[9] K. Zhang, Z. H. Jiang, W. Hong and D. H. Werner, "A low-profile and wideband triple-mode antenna for wireless body area network concurrent on-/off-body communications," *IEEE Trans. Antennas Propag.*, vol. 68, no. 3, pp. 1982-1994, Mar. 2020.

[10] X. Jiang, Z. Zhang, Y. Li and Z. Feng, "A novel null scanning antenna using even and odd modes of a shorted patch," *IEEE Trans. Antennas Propag.*, vol. 62, no. 4, pp. 1903-1909, Apr. 2014.

[11] S. N. Mastura Zainarry, S. J. Chen and C. Fumeaux, "A pattern-reconfigurable single-element microstrip antenna," in *Proc. RADIO*, Wolmar, Mauritius, Oct. 2018, pp. 1-2.

[12] H. Tian, K. Dhwaj, L. J. Jiang and T. Itoh, "Beam scanning realized by coupled modes in a single-patch antenna," *IEEE Antennas Wireless Propag. Lett.*, vol. 17, no. 6, pp. 1077-1080, Jun. 2018.

[13] F.-X. Liu, W. Dou, J. Cui, S. J. Chen and C. Fumeaux, "A concept of pattern-reconfigurable single-element antenna based on half-mode substrate-integrated cavity," in *Proc. EuCAP*, Copenhagen, Denmark, Mar. 2020, pp. 1-4.

[14] F.-X. Liu, T. Kaufmann, Z. Xu and C. Fumeaux, "Wearable applications of quarter-wave patch and half-mode cavity antennas," *IEEE Antennas Wireless Propag. Lett.*, vol. 14, pp. 1478–1481, 2015.

[15] M. K. Magill, G. A. Conway and W. G. Scanlon, "Tissue-independent implantable antenna for in-body communications at 2.36–2.5 GHz," *IEEE Trans. Antennas Propag.*, vol. 65, no. 9, pp. 4406-4417, Sep. 2017.

[16] S. J. Chen, T. Kaufmann, D. C. Ranasinghe and C. Fumeaux, "A modular textile antenna design using snap-on buttons for wearable applications," *IEEE Trans. Antennas Propag.*, vol. 64, no. 3, pp. 894-903, Mar. 2016.